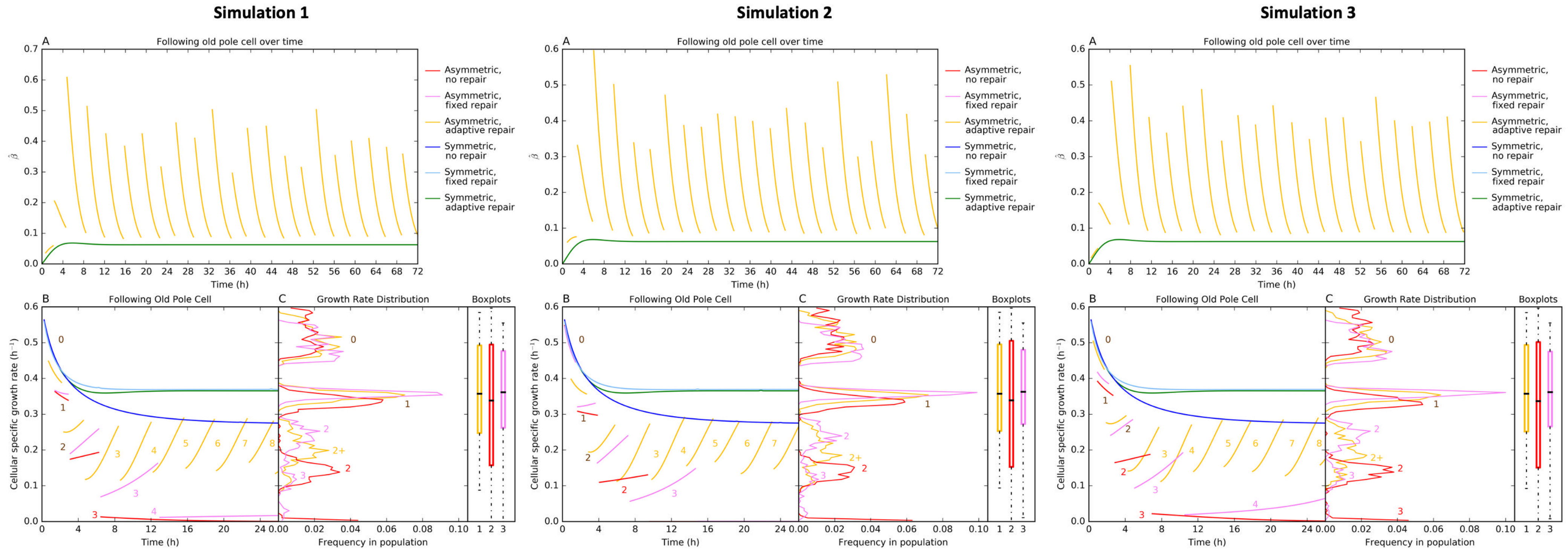

Figure 2 replicate simulations. Characteristics of strategies in a constant environment (no competition). **(A)** Investment into repair ($\hat{\beta}$ on the y axis) for the new adaptive repair strategy following the old pole cell over many divisions. In asymmetric divisions, the old pole cell inherits all damage, leading to a jump in allocation into repair following division and then decreasing steadily until the next division. In symmetric divisions, damage, and therefore investment into repair, reaches a steady state. **(B)** Specific growth rate of a single cell over consecutive cell divisions. Numbers in the panel label generations and each generation is shown with a new line (for asymmetric strategies). The specific growth rate of an asymmetrically dividing cell with no repair (red, $\beta = 0$) drops quickly to zero. For a cell with fixed optimal repair (magenta, $\beta = 0.07$), it decreases more slowly over time but also reaches zero. For a cell with adaptive repair (yellow, $\hat{\beta}$ variable), it decreases only initially towards a see-saw pattern, as in (A). Specific growth rates do not change at division for symmetric strategies (blue, cyan, and green) and there is no difference between daughter cells. Symmetric strategies show an initial decrease in specific growth rate before reaching a steady state, with similar values for fixed and adaptive repair and lower without repair. **(C)** Distribution of specific growth rates in populations at steady state (snapshot taken at 100 days) for asymmetrically dividing cells. Specific growth rates of cells with adaptive repair are between those with fixed repair and those without repair. The medians and inter-quartile ranges for adaptive and fixed repair are close and higher than for symmetrically dividing cells. Data are reproduced with permission from Fig. 5A,B in Clegg *et al.* (2014) (46), with the new adaptive repair strategy added. Specific growth rate was 0.6 h^{-1} and aging rate was 0.22 h^{-1}/μ_G and dependent upon specific growth rate for all strategies. Simulation 1 is shown in the main text (Fig. 2).

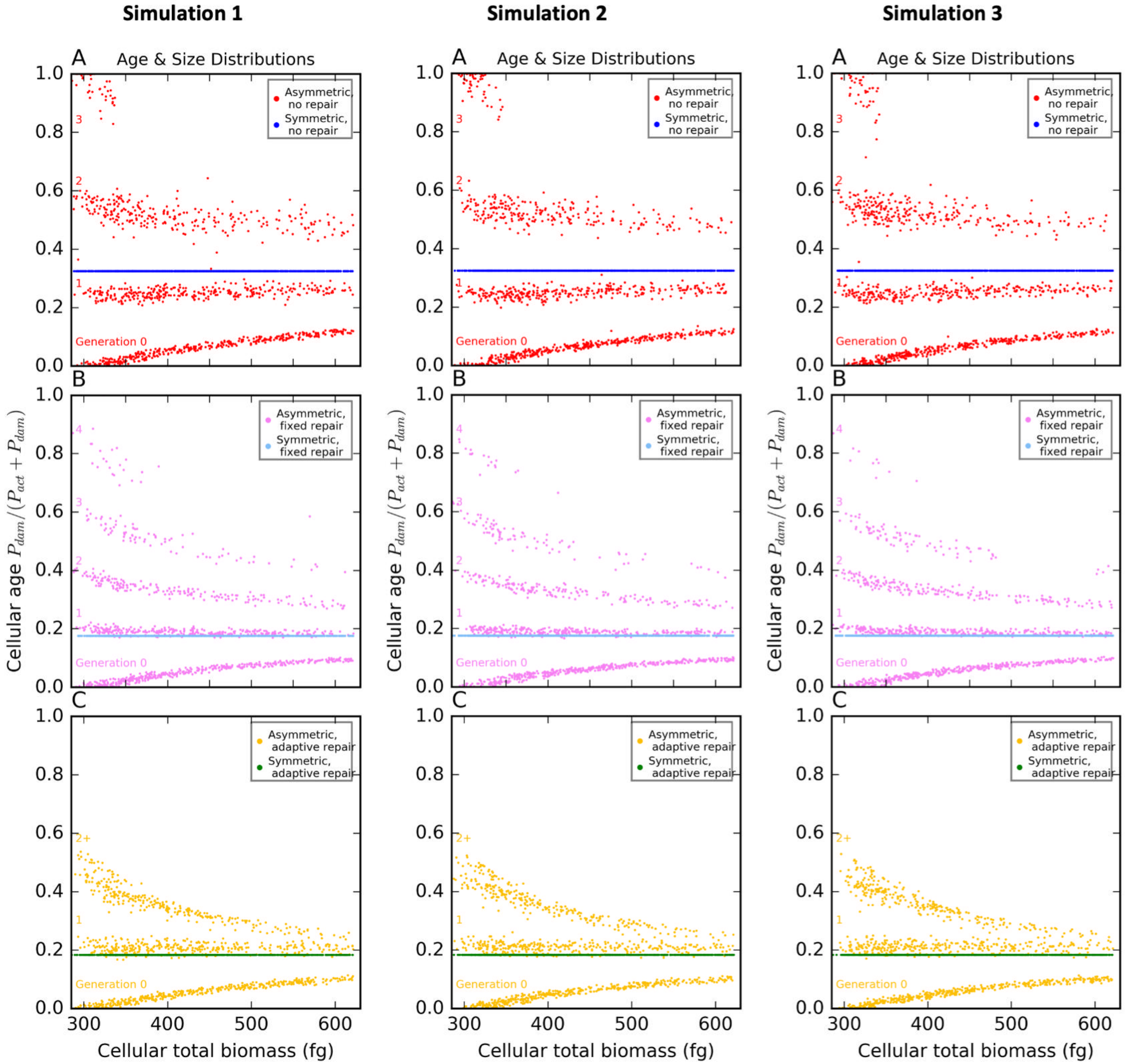

Figure 3 replicate simulations. Age and size distributions of populations in a constant environment (snapshot at 100 days, after reaching steady state). **(A)** Strategies without repair, **(B)** strategies with fixed repair and **(C)** strategies with adaptive repair. For symmetric division, cells without repair were substantially older than cells with fixed or adaptive repair, which were of similar age. For asymmetric division, the age of cells with adaptive repair stays well below the maximum age of one and reaches this level from generation three onwards so there are fewer very old cells than for fixed repair or without repair. Repair reduces the age of older cells over the cell cycle. The largest cells are approaching the division threshold, P_{div}, of 620 fg. Data are reproduced with permission from Fig. 5C,D in Clegg *et al*. 2014 (46), with the addition of the new adaptive repair strategy. Specific growth rate was 0.6 h^{-1} and aging rate was 0.22 h^{-1}/μ_G and dependent upon specific growth rate for all strategies. Simulation 1 is shown in the main text (Fig. 3).

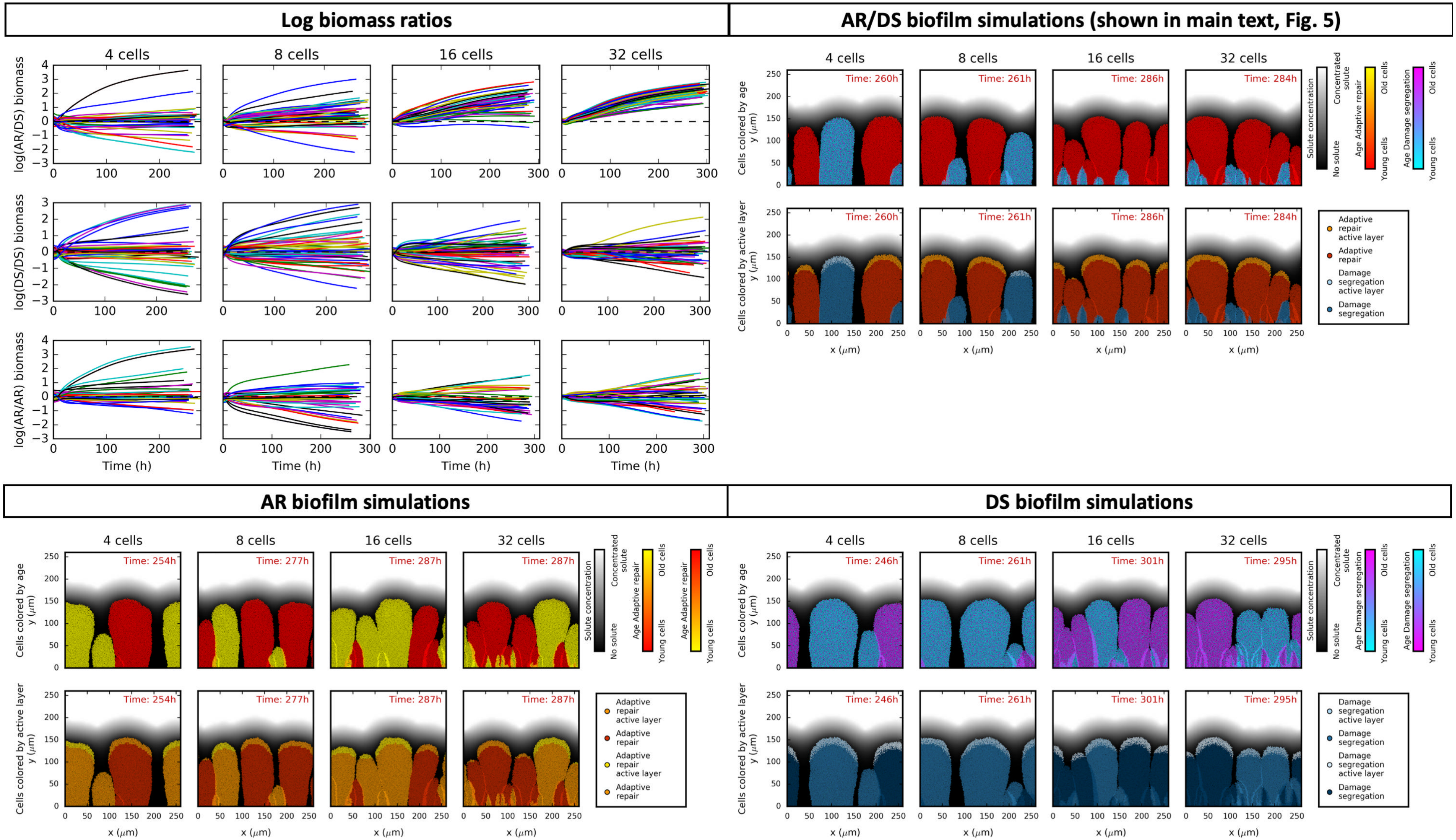

Control simulations for Fig. 6. Competitions between adaptive repair and damage segregation strategies and controls. Time courses of log biomass ratios (top) and biofilm structures at the last time point of the simulations (bottom). The higher the initial cell density, the more advantageous adaptive repair (AR) became, compared with damage segregation (DS). Control competitions were closer the higher the initial cell density was for both AR and DS. Panels from left to right show competitions initialized with 4, 8, 16 or 32 cells. (Top) Time courses of 50 replicate biofilm competitions between two strategies are shown using log biomass ratios to make the horizontal line at log(ratio) = 0 a symmetry axis. (Bottom) Cells are colored either by age or by position within the active layer of rapidly growing cells, defined as cells with a specific growth rate within 5% of the highest specific growth rate of a cell at the last time point of the simulation. Maximum specific growth rate was 1.2 h^{-1} and specific growth rate dependent damage accumulation rate was set at 0.22 h^{-1}/μ_G. Statistics for these competitions are shown in Table S1, mean biomass ratios at the end of competitions are shown in Figure 6 and results of replicate simulations are shown in figures in the file at 10.6084/m9.figshare.11520534.